A Tool to Enable Intraoperative Insertion Force Measurements for Cochlear Implant Surgery

Georg Böttcher-Rebmann, Viktor Schell, Leon Budde, M. Geraldine Zuniga, Claas Baier, Thomas Lenarz, and Thomas S. Rau

Abstract*—*Objective: **Residual hearing preservation during cochlear implant (CI) surgery is closely linked to the magnitude of intracochlear forces acting during the insertion process. So far, these forces have only been measured in vitro. Therefore, the range of insertion forces and the magnitude of damage-inducing thresholds in the human cochlea in vivo remain unknown. We aimed to develop a method to intraoperatively measure insertion forces without negatively affecting the established surgical workflow. Initial experiments showed that this requires the compensation of orientation-dependent gravitational forces.** ***Methods:*** **We devised design requirements for a force-sensing manual insertion tool. Experienced CI surgeons evaluated the proposed design for surgical safety and handling quality. Measured forces from automated and manual insertions into an artificial cochlea model were evaluated against data from a static external force sensor representing the gold standard.** ***Results:*** **The finalized manual insertion tool uses an embedded force sensor and inertial measurement unit to measure insertion forces. The evaluation of the proposed design shows the feasibility of orientation-independent insertion force measurements. Recorded forces correspond well to externally recorded reference forces after reliable removal of gravitational disturbances. CI surgeons successfully used the tool to insert electrode arrays into human cadaver cochleae.** ***Conclusion:*** **The presented positive evaluation poses the first step towards intraoperative use of the proposed tool. Further in vitro experiments with human specimens will ensure reliable in vivo measurements.** ***Significance:*** **Intraoperative insertion force measurements enabled by this tool will provide insights on the relationship between forces and hearing outcomes in cochlear implant surgery.**

***Index Terms*—Cochlear implant, gravity-independent force measurement, insertion forces, intraoperative insertion force measurement, manual insertion tool.**

Manuscript received 17 June 2022; revised 11 November 2022; accepted 14 November 2022. Date of publication 24 November 2022; date of current version 21 April 2023. This work was supported in part by the Federal Ministry of Education and Research of Germany (BMBF), under Grant 13GW0367B, and in part by Deutsche Forschungsgemeinschaft (DFG, German Research Foundation) under Germany's Excellence Strategy – EXC 2177/1 – under Project 390895286. The cochlear catheters were provided by MED-EL (*MED-EL Elektromedizinische Geräte Gesellschaft m.b.H., Innsbruck, Austria). (Corresponding author: Georg Böttcher-Rebmann.)*

Georg Böttcher-Rebmann is with the Department for Otorhinolaryngology, Head and Neck Surgery and Cluster of Excellence EXC 2177/1 "Hearing4all", Hannover Medical School, 30625 Hannover, Germany (e-mail: boettcher.georg@mh-hannover.de).

Viktor Schell, M. Geraldine Zuniga, Thomas Lenarz, and Thomas S. Rau are with the Department for Otorhinolaryngology, Head and Neck Surgery and Cluster of Excellence EXC 2177/1 "Hearing4all", Hannover Medical School, Germany.

Leon Budde is with the Institute of Mechatronic Systems, Leibniz University Hannover, Germany.

Claas Baier is with the Institute for Medical Microbiology and Hospital Epidemiology, Hannover Medical School, Germany.

Digital Object Identifier 10.1109/TBME.2022.3224528

I. Introduction

THE preservation of residual hearing capabilities is a major focus in cochlear implant (CI) research in the past decade. The remaining natural hearing can improve speech recognition in background noise, localization, music perception and reportedly quality of life [1], [2]. The preservation of this residual hearing has been closely linked to the degree of intracochlear trauma inflicted during CI surgery [3], [4]. A parameter consistently reported to impact intracochlear trauma is the magnitude of forces that the electrode array (EA) exerts upon the intracochlear tissue during insertion. If these forces are too high, intracochlear structures like the basilar membrane, dividing the scala tympani and the scala vestibuli, can be disrupted, which can lead to loss of the residual hearing and suboptimal hearing outcomes. Due to the microscopic dimensions and delicate nature of the inner ear, threshold forces to prevent damage are relatively small. Trauma-inducing forces as little as 42 mN have been reported [5] with even lower values for singular risk structures such as the basilar membrane (26–35 mN) and Reissner's membrane (4.2 mN) [6].

Due to the relevance of this issue, many studies aim at the investigation of insertion forces. Multiple approaches were devised to measure these forces. A common measurement method shown in Fig. 1(a) utilizes external sensors connected to either an artificial cochlea model (ACM) or a temporal bone (TB) specimen. In most studies, the force sensor is placed underneath the cochlea to measure forces acting on the cochlea as a whole during insertion [7], [8], [9], [10]. Recently, an ACM with a force sensitive artificial basilar membrane has been developed, which allows a simplified differentiation between general insertion forces and forces acting on the basilar membrane [11].

While these approaches are suitable for the in vitro analysis of insertion forces, they cannot be used to measure the insertion forces acting during surgery as no external force sensor with the required precision can be attached to the patient. Therefore, surgeons have to rely on their haptic perception of insertion forces. Kratchman et al. found that the median human perception

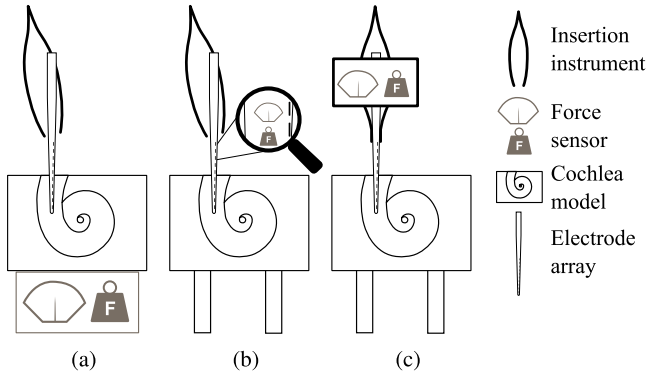

Fig. 1. Methods to measure EA insertion forces: Under the cochlea or ACM (a), inside the EA (b), inside the EA holding tool (c).

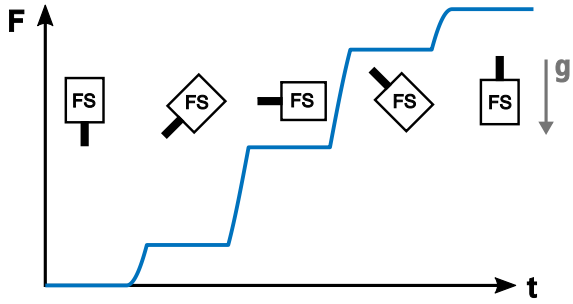

Fig. 2. Influence of gravity on measured force. Force sensor (FS) with attached mass (black bar) oriented with respect to gravity (grey arrow). Scale of measured force depends on attached mass.

threshold during the electrode array insertion is at 20.4 mN with a range of 10.8 mN to 36.5 mN and a reaction time between 100 ms and 200 ms [12]. Critical forces are thus close to imperceptible and the haptic resolution is likely limited close to the perception threshold. Reliable in vivo insertion force measurements could serve to enhance the surgeon's perception by providing force feedback and thereby help prevent insertion trauma.

One possibility for in vivo insertion force measurements is the integration of force sensors into the EA itself as shown in Fig. 1(b). Wade et al. integrated an optical fiber with fiber-bragg-gratings into an EA [13]. This enables strain measurement at discrete points along the EA which can be translated to insertion forces. Using this system however requires its integration into a commercial EA without causing any disadvantages to the patient. To the best of our knowledge, such a system has not yet been approved for intraoperative use.

A different approach to measure insertion forces can be found in the context of insertion tools developed to enable linear insertions with slow, mechanically controlled speeds [14], [15]. Force feedback from external sensors was mostly used to monitor the insertion quality. In contrast, other systems have aimed at combining the actuation unit with an integrated force sensor (will be denoted as *internal* sensor in the following). Schurzig et al. fitted a custom aluminum frame with strain gauges to measure reactive forces acting on the EA [16], [17]. Miroir et al. integrated a one-dimensional force sensor between a linear actuator and the driven EA [18]. While these tools can be used in vitro, they are difficult to transfer into a surgical setting. The procedure would considerably vary from the standard manual insertion and the measured forces could differ from realistic insertion forces. Moreover, these tools are relatively complex and therefore not easily adaptable to comply with surgical sterility and safety guidelines.

Considering the presented methodology, there is currently no approach to characterize manual insertion forces during CI insertions. Therefore, the magnitude of in vivo insertion forces acting upon the cochlea is generally unknown. Measuring these forces can provide deeper insight into parameters influencing insertion trauma and help prevent it, which would be beneficial to residual hearing preservation. Moreover, knowledge about in vivo insertion forces can improve the development of ACM with realistic friction properties. This is vital in the design of new and improved EA as they are often tested through insertions into these models.

We propose a manual insertion tool with integrated force sensing capabilities to enable in vivo insertion force measurements. The presented design is adapted to surgical conditions and aims to enable first intraoperative insertion force measurements. As constant orientations cannot be assumed during manual use, orientation-dependent gravitational influences (see Fig. 2) need to be filtered from the force signal to enable reliable measurements.

As the term *insertion force* is often used imprecisely, we use the following distinction:

Intracochlear insertion forces: Forces acting between the EA and intracochlear tissue. These forces are often used to assess potential damage to the cochlea.

Perceived insertion forces: Forces perceived by the surgeon. While these include the intracochlear insertion forces, additional influences are present, such as friction at the round window or cochleostomy site or contact forces between the EA and anatomical structures inside the mastoidectomy. When interpreting the data, the difference between the total force and the actual intracochlear insertion force needs to be considered.

Subsequently, the *perceived insertion* forces are merely referred to as *insertion forces* as these are the forces that are measurable with the proposed insertion tool.

In this work, we devise design requirements for a manual insertion tool and present the resulting design choices. The proposed manual insertion tool is then evaluated in three experimental trials in terms of measurement quality and its compatibility with the standard surgical workflow. An algorithm for the compensation of gravitational influences is formulated and the quality and necessity of such a compensation is evaluated.

II. Material and Methods

A. Compensation of Gravitational Influence on the Force Signal

When measuring forces, a sensor is susceptible to the influence of gravity. For static orientations this influence is constant and can be leveled out. However, as the proposed tool

is designed for manual use, constant orientations cannot be assumed. Therefore, the gravitational influence depends on the variable orientation and needs to be considered when measuring forces. A possible solution to track this error is to measure the gravitational acceleration a in the direction of the force sensor. Signal noise due to quick movements can be neglected as the target application requires slow and steady motion.

The total signal of the force sensor F_S can be divided into three components: A constant bias F_B depending on the sensor's pre-defined zero point, a force F_a caused by gravitational acceleration along the sensor axis and the external forces F_E intended to be measured. The decomposed total measured signal then becomes

$$F_S(t) = F_B + F_a(t) + F_E(t). \tag{1}$$

The gravitational force F_a can be further decomposed into the acceleration a along the sensor axis and the accelerated mass m_a, which can be determined experimentally. The constant bias can be removed from the signal by recording a zeroing force F_0 and subtracting it from the measurement to even out an initial measurement offset. This force consists of the bias F_B and the gravitational force at the zeroing time $F_{a,0} = m_a \cdot a_0$. Using $F_0 = F_B + F_{a,0}$, the bias can therefore be computed as

$$F_B = F_0 - F_{a,0} = F_0 - m_a \cdot a_0. \tag{2}$$

The variable gravitational force is accounted for by subtracting a time-dependent gravitational term $F_a(t) = m_a \cdot a(t)$. Combining these compensation forces, the external forces can be computed as

$$\begin{aligned} F_E(t) &= F_S(t) - F_B(t) - F_a(t) \\ &= F_S(t) - F_0 + F_{a,0} - F_a(t) \\ &= F_S(t) - F_0 - m_a \cdot (a(t) - a_0)\,. \end{aligned} \tag{3}$$

B. Tool Design

Our approach to address the presented challenges was to design an insertion tool that provides live insertion force readings during CI electrode insertion. We first derived constitutive requirements for such a tool to ensure a methodical design process. These requirements are derived from literature as well as advisory by CI surgeons.

- Measurement of axial insertion forces with:
  - Expected peak forces of up to 200 mN
  - A resolution in the range of 1–2 mN
- Measurements independent of spatial orientation to allow free movement
- Mechanism to grasp the EA, locked connection during insertion, detachable afterwards
- Compatibility with different types of electrode array
- Sterility concept protecting the patient from intraoperative contamination
- Simple design allowing surgical handling and workflow integration
- Overall size that does not impair the surgeon's field of view during insertion

Following these requirements, an iterative design process was performed using computer-aided design (CAD) software (*Inventor Professional 2019, Autodesk Inc., San Rafael, CA, USA*). Design iterations were tested through rapid prototyping using a *Form 3B* (*Formlabs Inc., Somerville, MA, US*).

C. Experimental Validation: Measurement Quality

Following the completion of the tool's design, two types of experiments were conducted to evaluate the quality of insertion force measurements obtained with the proposed tool. A custom-made EA dummy was inserted into an ACM. The EA dummy was comprised of a cochlear catheter (*MED-EL Elektromedizinische Geräte Gesellschaft m.b.H., Innsbruck, Austria*) with a superelastic NiTi wire within the inner lumen. The wire had a diameter of 0.2 mm. The ACM used was milled into PTFE with a transparent PMMA cover to enable observation of its interior (previously described in [19]). The cochlea geometry used was obtained from a Micro CT scan of a TB sample.

An additional force sensor (*KD24 s*, *ME-Meßsysteme GmbH, Hennigsdorf, DE*) was placed below the ACM to obtain reference data to compare with the forces recorded with the tool, as such an external sensor placement is the current gold standard method for insertion force measurements.

Trial I: Automated ACM Insertion: In the first set of experiments, the tool was attached to a linear actuator driving the insertion. This enabled a controlled insertion with constant speed, constant orientation and a linear direction. The insertion was started with the tip of the EA dummy 1 mm above the ACM, accelerated with 1 $\frac{\text{mm}}{\text{s}^2}$, actuated with 0.2 $\frac{\text{mm}}{\text{s}}$ and stopped at an insertion depth of 17 mm which corresponds to an approximate insertion angle of 330°. The principal measurement axes of the force sensor within the tool and the sensor below the ACM were aligned to create equivalent settings for both measurements. Twenty-five insertions were performed in this experiment.

Trial II: Manual ACM Insertion: For the second set of experiments, the insertions were performed manually to provide a more realistic insertion setting. The rest of the setup remained equal to the automated insertion experiment. Likewise, the relation between the internally and externally measured forces could be observed. Moreover, first conclusions on the feasibility of manual insertions with the proposed tool and the performance of the orientation compensation could be drawn. As in the automated insertion experiment, twenty-five insertions were performed. The experimental setup for both sets of experiments is shown in Fig. 3(a) and (b). Two specific parameters were used to evaluate the recorded data:

Measurement Agreement: The Bland and Altman analysis was used to evaluate the agreement between the two sensors based on the correlation between the sensors and their difference across the measurement range [20]. Additionally, linear regression was used to identify constant or proportional offsets and the difference between the sensor values was plotted over the mean value between both at each data point. The visualization algorithm was adapted from [21].

Gravity Compensation Magnitude: As the range of motion during insertion is generally unknown, the need for

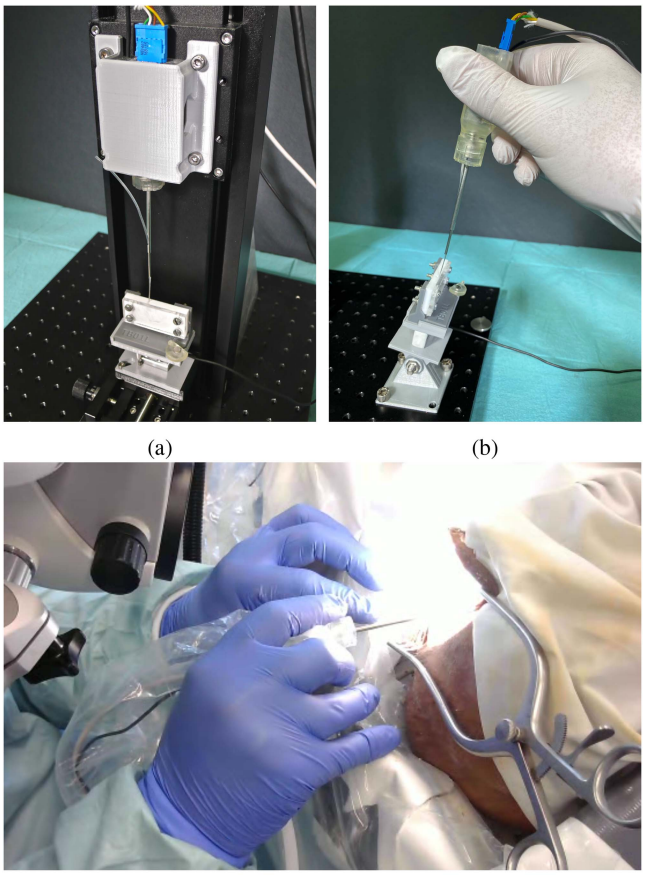

Fig. 3. Experimental setups: Automated (a), manual (b) and surgical evaluation (c).

compensation of gravitational influences on the force signal is uncertain. The magnitude of this compensated force depends on the change in orientation with respect to the gravitational axis. The peak of the gravitation-induced force is investigated for each trial to assess the need for such compensation. Following (3), this force is defined as

$$F_{a,max} = \max\left(|F_a(t)|\right) = \max\left(|m_a \cdot (a(t) - a_0)|\right). \quad (4)$$

D. Experimental Validation: Surgical Workflow

An experienced CI surgeon performed 15 EA insertions using a human cadaver head to assess the feasibility of the proposed surgical workflow. The goal of these trials was the evaluation of the visibility of relevant anatomical landmarks such as facial recess and the round window throughout the procedure. Moreover, the surgeon qualitatively evaluated the sterility concept and the handling of the tool. The surgical situation was simulated to be as realistic as possible in order to identify obstacles or possible improvements to be addressed before transition to live surgery. During the insertions, a first camera captured the surgeon's field of view through the surgical microscope and a second one recorded the hand holding the tool. The second camera perspective is visible in Fig. 3(c). Due to the typical limitations of formalin-fixed cadaveric specimens such as higher friction

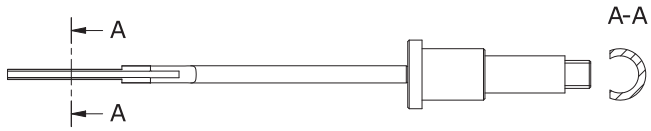

Fig. 4. Electrode array holder assembly with the main holder (left) and the threaded connector (right).

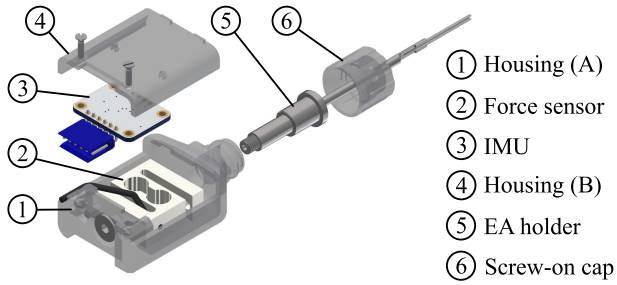

Fig. 5. Explosion view of the assembled tool.

forces and therefore shallower insertion depths, the alteration of intracochlear properties due to multiple insertions as well as the lack of a reference force sensor, the forces measured during these insertions were not evaluated.

III. Results

A. Tool Design

Sensors: For the force measurement, a unidirectional force sensor (*KD24 s, ME-Meßsysteme GmbH, Hennigsdorf, DE*) was selected, as it provides the desired force range ($\pm$ *2 N*) and precision (*up to* $\pm$ *0.2 mN*), is commercially available and has previously been used to measure in vitro insertion forces. The signal was amplified and recorded using a measurement amplifier (*GSV-4, ME-Meßsysteme*).

An Inertial Measurement Unit (IMU) was integrated (*BNO055, Bosch Sensortec GmbH, Reutlingen, DE*) to measure and compensate orientation-dependent gravitational influences on the forces. The IMU was oriented such that its Y-axis coincides with the force sensor's measurement axis.

Electrode Array Holder: The basic concept of an EA holder is adapted from previous work in our laboratory [22]. It is comprised of a U-shaped stainless steel half-tube with an inner radius fit to a specific electrode array. In this case it was adapted to the *MED-EL Flex series*. In order to connect the holder to the force sensor for direct force transmission, it is extended with an external M5x0.8 thread at the proximal end, which enables a direct connection between both. The EA holder is depicted in detail in Fig. 4.

Housing and Surgical Safety: A housing was designed to both provide an interface for the surgeon to hold the sensing unit and to enable sterile surgical handling by shielding the sensors from the intraoperative environment. The complete manual insertion tool is depicted in Fig. 5.

Given the inability to sterilize the sensors and the need to connect the force sensor to the sterile EA holder, a strategy

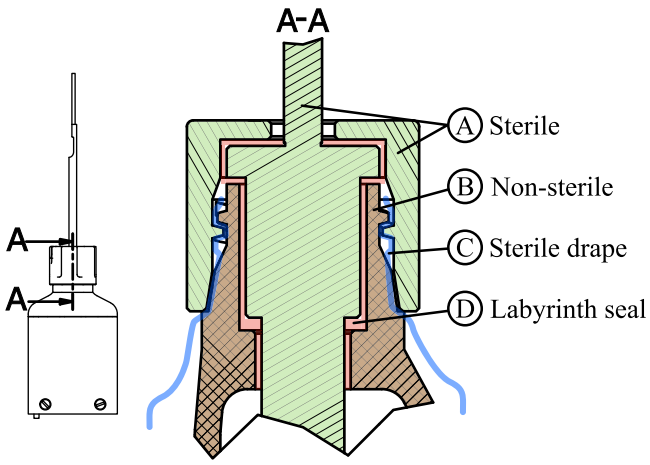

Fig. 6. Sterility design measures in the tool: Sterile parts (green) and non-sterile parts (orange) separated by sterile drape (blue) and labyrinth seal (red).

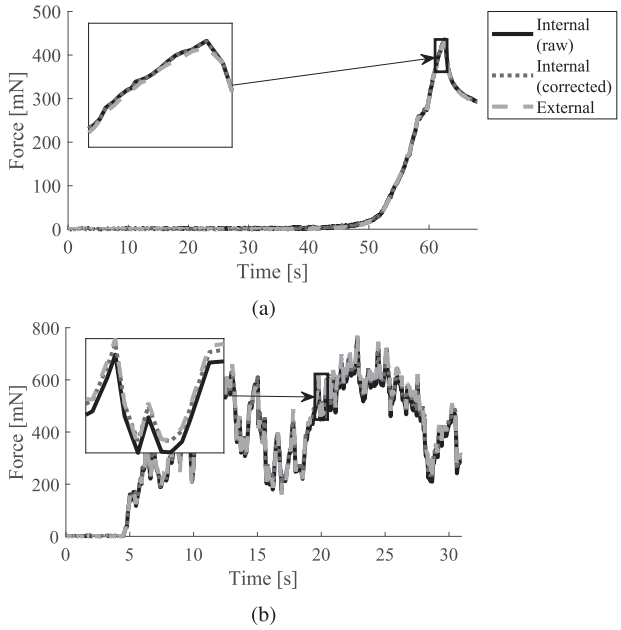

Fig. 7. Exemplary comparison between internally and externally measured insertion force in the first experiment in Trial I: Automated ACM Insertion (a) and Trial II: Manual ACM Insertion (b).

to shield off these two conflicting areas within the tool was developed. It is based on the use of a sterile drape, usually used to cover non-sterile endoscopes. The non-sterile sensor and its housing are covered with the drape with just a small hole adapted to the housing's outlet to allow the insertion of the EA holder without exposing non-sterile parts. The clamping section of the holder is oriented such that it points toward the tool's narrow side. That way, the EA can be released in the caudal direction while providing maximum visibility during insertion. The drape is subsequently fixed to the housing with a sterile screw-on cap to ensure that all sections stay covered. The clearings between the EA carrier, the housing and its cap are dimensioned as small as possible without inducing contact between the both to minimize possible contamination between the internal tool volume and the intraoperative exterior. Additionally, the clearings are arranged to form a labyrinth seal. These measures prevent substances from entering the tool as well as particles from dropping out. A visualization of the sterility design measures is shown in Fig. 6.

Software: A software tool was implemented to record the sensor data with up to 100 Hz, synchronize the data sources with respect to each other, compute the gravity compensation and visualize the measurements. It was developed in C++ using the QT 5.12.9 framework (*The QT Company, Espoo, Finland*). The recording of up to two videos synchronous to the data provides the possibility to correlate data anomalies to specific phenomena visible in the videos.

B. Experimental Validation: Measurement Quality

The data gathered in the experimental trials was used to assess the quality of measurements with the proposed tool.

Measurement Agreement: In both insertion trials, all 25 insertions were successfully performed with full EA insertions. Fig. 7(a) and (b) exemplarily show the measured insertion forces for a single insertion for each trial. Although a difference between internally and externally recorded forces can hardly be distinguished in the plot, the different force profiles for a manual and an automated insertion become evident.

The agreement between the signals is further illustrated in correlation plots and Bland-Altman plots. The correlation plot in Fig. 8(a) shows no systematic difference between the internal and external signal for the automated ACM insertion trial. The median force difference between the internal and external signal is shown in the corresponding Bland-Altman diagram. For all automated insertions, a signal difference of 0.6 mN with an interquartile range of 3.3 mN can be observed. The more extreme outliers are rooted in singular trials and especially occurred toward the end of the insertion. These results are the same with and without gravity compensation, showing that the compensation does not negatively affect the measurement.

Fig. 8(b) shows the correlation and Bland-Altman plots for the manual insertion trial. A slightly reduced correlation between the internally and externally recorded forces can be observed. The median force difference between the two signals for all manual insertions is -3.2 mN with an interquartile range of 12 mN. These values describe the difference between the external sensor and the tool sensor without gravity compensation. Fig. 8(c) shows the data with active gravity compensation for the internally recorded forces. With this compensation, the median force difference between the signals is reduced to -0.5 mN with an interquartile range of 7.9 mN. While the corresponding correlation line equation shows a slope slightly closer to 1, it exhibits a small bias toward the internally recorded forces visible in the y intercept.

Gravity Compensation Magnitude: The peak forces induced by gravitation are shown in Fig. 8(e). For the first experimental trial a median value of 0.8 mN with an interquartile range of 0.1 mN can be observed. For the second trial these values increase to a median of 7.9 mN with an interquartile range of 2.8 mN.

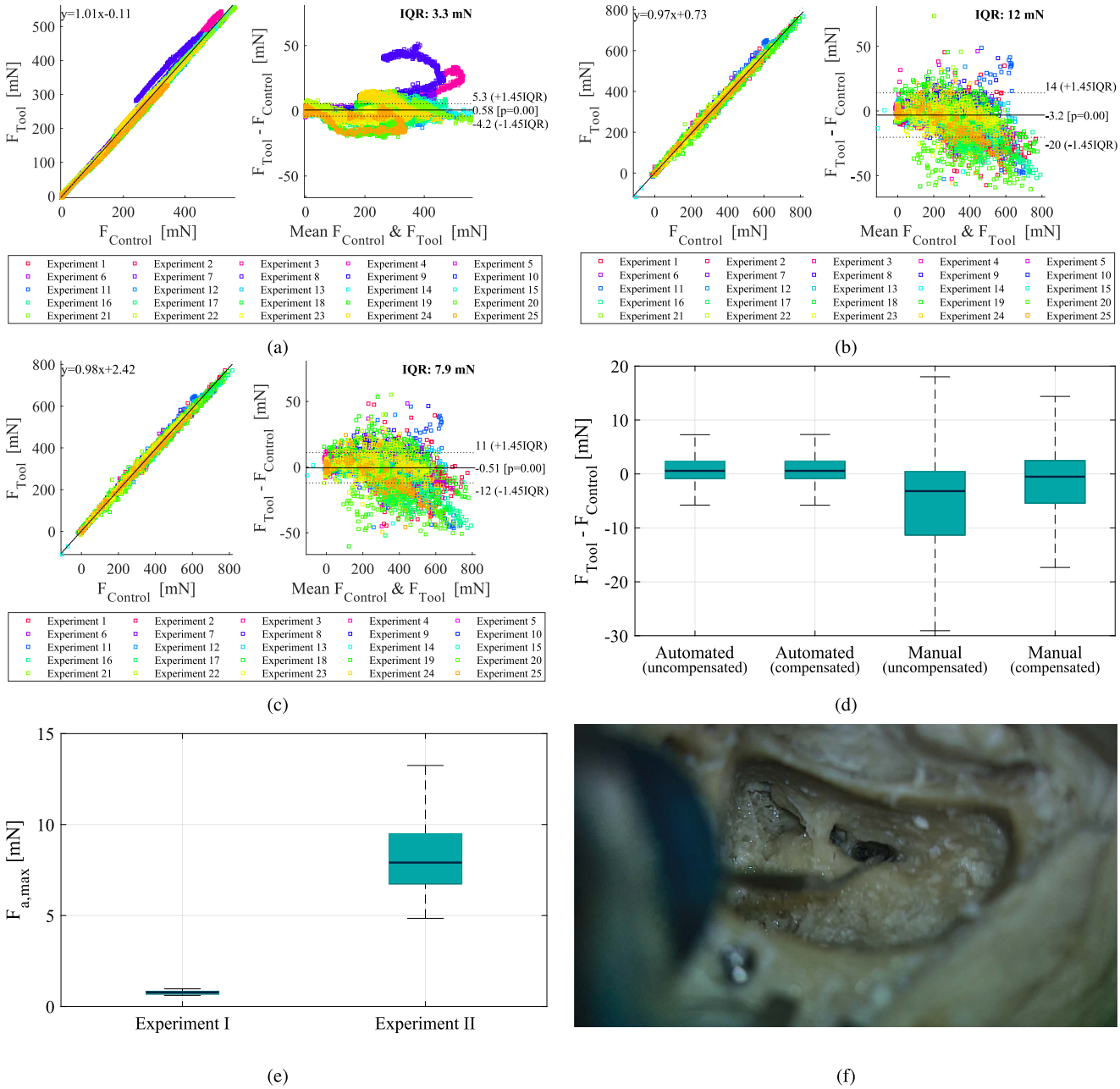

Fig. 8. Experimental validation results. Correlation and Bland-Altman plots of the automated insertions (a), the manual insertions without (b) and with gravity compensation (c). Boxplot of the absolute differences between internal and external force sensor for both trials with and without gravity compensation (d). Gravity compensation magnitude for both trials (e). Surgeon's field of view seen through an OR microscope (f).

C. Experimental Validation: Surgical Workflow

During all 15 insertions, the tool did not obstruct the visibility of relevant anatomical structures. If necessary, the line of sight can be almost parallel to the EA holder, between 5.4° and 7.6° depending on insertion depth. An exemplary field of view from the OR microscope used is shown in Fig. 8(f). The connection between the tool and the sterile drape remained stable during all trials. Moreover, no breaches in the drape surface that could have violated the sterile field were observed. The obtained insertion depth was equal to the insertion depth achieved with the conventional insertion method using a surgical forceps.

IV. Discussion

The evaluation shows that the proposed design for a manual insertion tool provides the desired functionality. Insertion forces can be measured in the desired range and are reliably corrected for gravity-induced artefacts.

Experimental Results: When comparing the internally and externally recorded forces in the automated ACM insertion trial, a good correlation between the two can be observed. With the exception of some peaks in force differences for particular insertions that were observed mainly toward the end of the respective insertion, the force differences were steadily low. This

is highlighted by the small median force difference of 0.6 mN and the interquartile range of 3.3 mN. When considering comparable approaches, only Miroir et al. have similarly compared an internal to an external force sensor. The mean force difference reported is 10 ± 1 mN with a visibly lower correspondence between the two signals [18]. These experiments are comparable to ours as in both the internal force sensor is linearly translated, causing an insertion into a cochlea connected to an external sensor. This improved measurement accuracy highlights the proposed design's potential suitability for intraoperative measurements.

When examining the manual ACM insertion trial, the agreement between the two sensors is still satisfactory, but the increased interquartile range in the sensor differences suggests a higher noise present in the measurements. A possible reason for this is the variable tool orientation which can introduce insertion forces with components perpendicular to the external sensor's measurement axis. These components would not be accounted for in the external sensor's signal, however they would be present in the insertion tool's measurement. As these perpendicular components can both increase and decrease the difference between the sensors, they do not cause a systematic offset but rather an increased measurement noise.

Moreover, the EA dummy used in the experiments has to be considered. While the superelastic NiTi wire heavily increases its reusability as there is no permanent deformation after an insertion, the stiffness is comparably high. Forces in a setting with realistic cochlea properties and typical low-stiffness EAs are expected to be significantly lower. This would lead to an additional reduction of the aforementioned artifacts. The presented force differences can therefore be regarded as a conservative estimate of force differences for the proposed insertion tool.

The investigation of the implemented gravity compensation allows two conclusions. First, the algorithm successfully uses the IMU signal to correct the orientation-dependent raw forces measured in the tool. This is visible in Fig. 8(d) as the median force differences are reduced through gravity compensation. The second conclusion can be drawn from the gravitation compensation magnitude visualized in Fig. 8(e). For a manual insertion force measurement, orientation-dependent forces above 10 mN are present. While these seem small in comparison to the presented insertion forces, these are comparably high due to the used EA dummy and the ACM. With a realistic EA and live tissue, the insertion forces are expected to be an order of magnitude smaller while the orientation-dependent forces would remain the same. Considering these dimensions, orientation-dependent forces around 10 mN would substantially reduce the measurement's quality. Gravity compensation is thus essential for successful manual insertion force measurements.

Therefore, both experimental trials show that the proposed insertion tool is able to measure insertion forces equivalently to a sensor placed underneath the cochlea, which constitutes the current gold standard in insertion force measurements.

Design and Surgical Workflow Assessment: The performed insertions show that using the insertion tool does not impair the surgical workflow with respect to the conventional approach. The surgeon intuitively integrated the tool into their routine procedures.

As this work aims to validate the functionality of the proposed insertion tool, interpreting recorded data in the anatomical context exceeds the scope. A first evaluation was presented in [23].

Limitations: The EA dummy was used multiple times in the experiments. While the NiTi wire restores the shape, some deterioration over time is to be expected. Therefore, not all of the 25 insertions are comparable with respect to each other. Although a solution would be to use a new EA for each insertion, their availability and cost limits this approach. For a proof-of-concept, EA re-usage was therefore deemed sufficient.

In the presented experiments, no relationship between time and insertion depth can be drawn. Unlike automated insertions, where this can be easily studied, manual insertions complicate this analysis as only the orientation but not the absolute position in space can be measured by the IMU. The knowledge about insertion forces at a certain depth for a specific cochlea is a relevant parameter in insertion force research. For this purpose, the tool might be extended with tracking technology in future experiments.

During the surgical workflow validation experiments, potential sources for signal noise or distortion were identified. When the EA holder is in direct contact with bone, other tissue or any surgical instruments, unknown forces are introduced to the measurement. Similarly, strong manipulation of the EA with a forceps, e.g. to remove it from the EA holder results in additional forces recorded by the tool. Video recording of the insertion procedure can be beneficial to be able to detect such events and exclude the corresponding data.

In surgery, the EA is connected to a processor, which is already implanted when the insertion is performed. Due to limited lead length, this connection could also introduce unknown forces to the measurement. The extent of this effect will be investigated in future work to assess its relevance. However, first investigations showed little to no effect due to the small range of motion during the insertion.

The force measurement can be susceptible to temperature changes. While we do not expect the temperature to meaningfully fluctuate during our short measurement, the IMU is equipped with a temperature sensor, which would enable us to record temperature data for future experiments to rule out temperature affection of the signal.

V. Conclusion

The proposed design for an insertion force measurement tool to be used during conventional CI surgery proves to be suitable for its envisioned task. The measured and processed insertion forces correspond well to forces recorded with an external sensor and are therefore equivalent to the gold standard. The design has been evaluated and approved by experienced CI surgeons in terms of handling and surgical safety. Further preclinical testing will substantiate surgical handling experience and allow a first interpretation of in vitro insertion forces. Following the

necessary regulatory requirements, we aim to introduce the tool into the OR.

A development step parallel to collecting and evaluating intraoperative data will be extending the tool's functionalities. The IMU can also provide information on a surgeon's movements during the insertion. With more knowledge about insertion forces and angles, the measurements can be used to monitor the insertion process and warn of critical thresholds, similar to intraoperative electrocochleography [24]. Likewise, a live feedback system using a digital microscope as proposed in [25] can aid surgeons in optimizing insertion parameters such as speed or the insertion angle.

REFERENCES

[1] R. H. Gifford et al., "Cochlear implantation with hearing preservation yields significant benefit for speech recognition in complex listening environments," *Ear Hear.*, vol. 34, no. 4, pp. 413–425, Jul. 2013.

[2] C. Welch et al., "Electric and acoustic stimulation in cochlear implant recipients with hearing preservation," *Seminars Hear.*, vol. 39, no. 04, pp. 414–427, Nov. 2018.

[3] T. Lenarz, "Cochlear implant–State of the Art," *GMS CurrTop Otorhinolaryngol Head Neck Surg*, vol. 16, May 2017, Art. no. Doc04.

[4] M. L. Carlson et al., "Survey of the American Neurotology Society on cochlear implantation: Part 2, Surgical and device-related practice patterns," *Otol. Neurotol.*, vol. 39, no. 1, pp. e20–e27, Jan. 2018.

[5] D. Schuster et al., "Characterization of intracochlear rupture forces in fresh human cadaveric cochleae," *Otol. Neurotol.*, vol. 36, no. 4, pp. 657–661, 2015.

[6] T. Ishii et al., "Mechanical properties of human round window, Basilar and Reissner's membranes," *Acta Otol-Laryngol.*, vol. 115, no. sup519, pp. 78–82, Jan. 1995.

[7] C. A. Todd, F. Naghdy, and M. J. Svehla, "Force application during cochlear implant insertion: An analysis for improvement of surgeon technique," *IEEE Trans. Biomed. Eng.*, vol. 54, no. 7, pp. 1247–1255, Jul. 2007.

[8] T. S. Rau et al., "Automated insertion of preformed cochlear implant electrodes: Evaluation of curling behaviour and insertion forces on an artificial cochlear model," *Int. J. Comput. Assist. Radiol. Surg.*, vol. 5, no. 2, pp. 173–181, 2010.

[9] J. P. Kobler et al., "Cochlear dummy electrodes for insertion training and research purposes: Fabrication, mechanical characterization, and experimental validation," *BioMed Res. Int.*, vol. 2015, 2015, Art. no. 574209.

[10] P. Aebischer et al., "In-vitro study of speed and alignment angle in cochlear implant electrode array insertions," *IEEE Trans. Biomed. Eng.*, vol. 69, no. 1, pp. 129–137, Jan. 2022.

[11] C. M. Hendricks et al., "Magnetic steering of robotically inserted lateral-wall cochlear-implant electrode arrays reduces forces on the basilar membrane in vitro," *Otol. Neurotol.*, vol. 42, no. 7, pp. 1022–1030, Aug. 2021.

[12] L. B. Kratchman et al., "Force perception thresholds in cochlear implantation surgery," *Audiol. Neurotol.*, vol. 21, no. 4, pp. 244–249, 2016.

[13] S. A. Wade et al., "Measurement of forces at the tip of a cochlear implant during insertion," *IEEE Trans. Biomed. Eng.*, vol. 61, no. 4, pp. 1177–1186, Apr. 2014.

[14] S. Hügl et al., "Investigation of ultra-low insertion speeds in an inelastic artificial cochlear model using custom-made cochlear implant electrodes," *Eur. Arch. Oto-Rhino-Laryngol.*, vol. 275, no. 12, pp. 2947–2956, 2018.

[15] M. G. Zuniga et al., "The effect of ultra-slow velocities on insertion forces: A study using a highly flexible straight electrode array," *Otol. Neurotol.*, vol. 42, no. 8, pp. e1013–e1021, Sep. 2021.

[16] D. Schurzig et al., "A force sensing automated insertion tool for cochlear electrode implantation," in *Proc. IEEE Int. Conf. Robot. Automat.*, 2010, pp. 3674–3679.

[17] J. P. Kobler et al., "An automated insertion tool for cochlear implants with integrated force sensing capability," *Int. J. Comput. Assist. Radiol. Surg.*, vol. 9, no. 3, pp. 481–494, 2014.

[18] M. Miroir et al., "Friction force measurement during cochlear implant insertion: Application to a force-controlled insertion tool design," *Otol. Neurotol.*, vol. 33, no. 6, pp. 1092–1100, 2012.

[19] S. Hügl et al., "Impact of anatomical variations on insertion forces: An investigation using artificial cochlear models," *Curr. Directions Biomed. Eng.*, vol. 4, no. 1, pp. 509–512, 2018.

[20] D. G. Altman and J. M. Bland, "Measurement in medicine: The analysis of method comparison studies," *Statistician*, vol. 32, no. 3, 1983, Art. no. 307.

[21] R. Klein, "Bland-Altman and correlation plot," MathWorks File Exchange, Accessed: Feb. 2, 2021. [Online]. Available: https://www.mathworks.com/matlabcentral/fileexchange/45049-bland-altman-and-correlation-plot

[22] T. S. Rau et al., "A simple tool to automate the insertion process in cochlear implant surgery," *Int. J. Comput. Assist. Radiol. Surg.*, vol. 15, no. 11, pp. 1931–1939, Nov. 2020.

[23] M. G. Zuniga et al., "Illustrating orientation changes of the insertion trajectory during cochlear implant electrode array insertion," *Curr. Directions Biomed. Eng.*, vol. 7, no. 2, pp. 113–116, Oct. 2021.

[24] A. Buechner et al., "Clinical experiences with intraoperative electrocochleography in cochlear implant recipients and its potential to reduce insertion trauma and improve postoperative hearing preservation," *PLoS One*, vol. 17, no. 4, Apr. 2022, Art. no. e0266077.

[25] D. Arweiler-Harbeck et al., "Digital live imaging of intraoperative electrocochleography–First description of feasibility and hearing preservation during cochlear implantation," *Otol. Neurotol.*, vol. 42, no. 9, pp. 1342–1346, Oct. 2021.